

THE PROGENITORS OF CORE-COLLAPSE SUPERNOVAE SUGGEST THERMONUCLEAR ORIGIN FOR THE EXPLOSIONS

DORON KUSHNIR¹

Draft version September 12, 2021

ABSTRACT

Core-collapse supernovae (CCSNe) are the explosions of massive stars following the collapse of the stars' iron cores. Poznanski (2013) has recently suggested an observational correlation between the ejecta velocities and the inferred masses of the red supergiant progenitors of type II-P explosions, which implies that the kinetic energy of the ejecta (E_{kin}) increases with the mass of the progenitor. I point out that the same conclusion can be reached from the model-free observed correlation between the ejected ^{56}Ni masses (M_{Ni}) and the luminosities of the progenitors for type II supernovae, which was reported by Fraser et al. (2011). This correlation is in an agreement with the predictions of the collapse-induced thermonuclear explosions (CITE) for CCSNe and in a possible contradiction with the predictions of the neutrino mechanism. I show that a correlation between M_{Ni} and E_{kin} holds for all types of CCSNe (including type Ibc). This correlation suggests a common mechanism for all CCSNe, which is predicted for CITE, but is not produced by current simulations of the neutrino mechanism. Furthermore, the typical values of E_{kin} and M_{Ni} for type Ibc explosions are larger by an order of a magnitude than the typical values for II-P explosions, a fact which disfavors progenitors with the same initial mass range for these explosions. Instead, the progenitors of type Ibc explosions could be massive Wolf-Rayet stars, which are predicted to yield strong explosions with low ejecta masses (as observed) according to CITE. In this case, there is no deficit of high mass progenitors for CCSNe, which was suggested under the assumption of a similar mass range for the progenitors of types II-P and Ibc supernovae.

Subject headings: supernovae: general

1. INTRODUCTION

There is strong evidence that supernovae of types II and Ibc are explosions of massive stars (e.g. Hirata et al. 1987; Arnett et al. 1989; van Dyk 1992; Smartt 2009), involving the collapse of the stars' iron cores and ejection of the outer layers. It is widely thought that the observed $\sim 10^{51}$ erg kinetic energy of the ejecta (E_{kin}) is due to the deposition of a small fraction ($\sim 1\%$) of the gravitational energy ($\sim 10^{53}$ erg) released in neutrinos (see Bethe 1990; Janka 2012, for reviews). So far, this scenario has not been demonstrated from first principles. In fact, one-dimensional simulations indicate that the neutrinos do not deposit sufficient energy. While some explosions were obtained in multi-dimensional simulations with simplified neutrino transport, the fundamental mechanism would only be satisfactorily demonstrated once accurate three-dimensional simulations, with all relevant physical process taken into account, become available. Burbidge et al. (1957) suggested a different mechanism for the explosion during core-collapse that does not involve the emitted neutrinos. In this proposed scenario, increased burning rates due to adiabatic heating of the outer shells as they collapse lead to a thermonuclear explosion (see also Hoyle & Fowler 1960; Fowler & Hoyle 1964). This collapse-induced thermonuclear explosion (CITE) naturally produces $\sim 10^{51}$ erg from thermonuclear burning of $\sim 1 M_{\odot}$ (gain of $\sim \text{MeV}/m_p$).

Kushnir & Katz (2014) have shown that CITE is possible in some (tuned) one-dimensional initial profiles, which include shells of mixed helium and oxygen, but resulting in weak explosions, $\lesssim 10^{50}$ erg, and negligible amounts of ^{56}Ni are ejected. In Kushnir (2015) I have recently used two-dimensional simulations of rotating massive stars to explore

the conditions required for CITE to operate successfully. I found out that for stellar cores that include slowly (a few percent of breakup) rotating $\sim 0.1 - 10 M_{\odot}$ explosive shells of He-O with densities of few $\times 10^3 \text{ g cm}^{-3}$, an ignition of a thermonuclear detonation that unbinds the stars' outer layers is obtained. With a series of simulations that cover a wide range of the progenitor masses and profiles, I showed that CITE is insensitive to the assumed profiles and thus a robust process that leads to supernova explosions for rotating massive stars. The resulting explosions have E_{kin} in the range of $10^{49} - 10^{52}$ erg, and ejected ^{56}Ni masses (M_{Ni}) of up to $\sim 1 M_{\odot}$, both of which cover the observed ranges of core-collapse supernovae (CCSNe, including types II and Ibc). CITE predicts that stronger explosions (i.e., larger E_{kin} and higher M_{Ni}) are from progenitors with higher masses. Testing if the required initial conditions for CITE to operate exist in nature is difficult observationally, but here I show observational evidence from CCSNe that are in agreement with the prediction that stronger explosions are from progenitors with higher masses, which implies that CITE may be the dominant mechanism for CCSNe explosions.

In recent years, direct identifications of the progenitors have been made for CCSNe in pre-explosion images, and they provide powerful tests for CCSNe theories (e.g. Smartt 2009; Leonard 2011; Smartt 2015). Several observed correlations between the properties of the progenitors and the supernovae suggest that more massive progenitors lead to stronger explosions. Poznanski (2013) has recently suggested an observational correlation between the ejecta velocities and the inferred masses of the red supergiant progenitors of type II-P explosions. The correlation implies that E_{kin} is approximately proportional to the mass of the progenitor cubed. Poznanski (2013) suggested that the same correlation can be also deduced for type II-P supernovae from the observed uni-

¹ Institute for Advanced Study, Einstein Drive, Princeton, NJ, 08540, USA, kushnir@ias.edu

formity of the light-curve plateau duration (Poznanski et al. 2009; Arcavi et al. 2012) and the correlation between the light-curve luminosities and ejecta velocities (Hamuy & Pinto 2002; Nugent et al. 2006). In Section 2, I point out that more massive progenitors leading to stronger explosions can be deduced in a model-independent way from the observed correlation between M_{Ni} and the progenitor luminosities. This observed correlation was first reported by Fraser et al. (2011) (see also a closely related correlation between M_{Ni} and the masses of the progenitors, suggested by Smartt et al. 2009). Unlike progenitor masses or E_{kin} , whose inferences rely upon models (massive star evolution models or complicated light-curve models, respectively) and thus are subjective to large systematics uncertainties due to model assumptions, both M_{Ni} and progenitor luminosities are model-free and can be directly derived from observations. Furthermore, these two quantities can be deduced for all type II explosions and are not restricted to type II-P supernovae. I reproduce the correlation between M_{Ni} and the progenitor luminosities with an updated data (Section 2.1) and show that it is in an agreement with the predictions of CITE (Section 2.2) and in a possible contradiction with the predictions of the neutrino mechanism (Section 2.3).

The use of M_{Ni} as an indicator for E_{kin} is based on an observed correlation between M_{Ni} and E_{kin} shown in Section 3. I demonstrate that this correlation holds for all types of CCSNe, including both types II and Ibc (Section 3.1). This universal correlation suggests a common explosion mechanism for all CCSNe, which is predicted for CITE, but it is not produced by current simulations of the neutrino mechanism (Section 3.2). Furthermore, the typical values of E_{kin} and M_{Ni} for type Ibc explosions are larger by an order of a magnitude from the typical values for type II-P explosions. This fact disfavors a similar mass range for the progenitors of these events, and suggests that the progenitors of type Ibc explosions are massive Wolf-Rayet (WR) stars (Section 3.3). Since WR stars have more massive cores and stripped envelopes, CITE predicts that they lead to stronger explosions and relatively low ejecta masses, both of which are consistent with observations. Progenitor studies that assume a similar mass range for the progenitors of type II-P and type Ibc supernovae suggest a deficit of high mass progenitors ($\gtrsim 20 M_{\odot}$) for CCSNe, and if true, it would imply that higher mass stars produce “failed supernovae” – weak explosions that are very faint (e.g., see Smartt 2009). However, if massive WR stars are the progenitors of type Ibc supernovae, there is no deficit of high mass progenitors for CCSNe (Smartt 2015).

2. EJECTED ^{56}Ni MASSES VERSUS THE LUMINOSITIES OF THE PROGENITOR

2.1. Observations

The observed correlation between M_{Ni} and the luminosities of the progenitors, which was reported by Fraser et al. (2011), is reproduced with updated data in panel (a) of Figure 1. The sample includes all supernovae from Smartt (2015), for which estimates of M_{Ni} are available in the literature, supplemented with SN 1987A and SN 1993J (see Table 1). A clear correlation over one order of magnitude for both M_{Ni} and for the luminosity of the progenitor is apparent, where the range of M_{Ni} roughly corresponds to $E_{\text{kin}} \sim \text{few} \times 10^{50} - \text{few} \times 10^{51}$ erg (see Figure 3). More luminous progenitors eject larger masses of ^{56}Ni . Note that SN 1987A and type IIb supernovae have the largest progenitors luminosities and the largest M_{Ni} values, a

property that will be discussed in Section 3.

It would seem natural to inspect the correlation between E_{kin} and the luminosity of the progenitors, rather than using M_{Ni} as an indicator for E_{kin} . The main motivation against using the inferred E_{kin} from observations is the complicated light-curve modeling that is involved for its estimation (which can include large systematic uncertainties), compared with the model-free determination of M_{Ni} . Indeed, only a weak correlation is obtained between the estimated E_{kin} reported in the literature (see Table 1) and the luminosity of the progenitors, as shown in Figure 2. The advantage of using M_{Ni} over E_{kin} is evident by comparing panel (a) of Figure 1 to Figure 2. The correlation between M_{Ni} and E_{kin} (Section 3) that is the justification for using M_{Ni} as an indicator for E_{kin} suffers as well from the large systematic uncertainties in the estimation of E_{kin} . However, in this case the sample is large and it spans more than two orders of magnitude in M_{Ni} and E_{kin} , such that the large systematic uncertainties are less important.

Since more luminous progenitors are more massive and since larger values of M_{Ni} imply larger E_{kin} , the correlation between M_{Ni} and the luminosities of the progenitors implies that more massive progenitors lead to stronger explosions, the same qualitative result found by Poznanski (2013). The model-free measurements of M_{Ni} and of the luminosities of the progenitors are more robust than the estimates of the masses of the progenitors (which depend on stellar evolution models) and of E_{kin} (which depend on complicated light-curve modeling). Furthermore, Poznanski (2013) used the Fe II $\lambda 5169$ absorption feature to estimate the velocity of the ejecta, which limits the analysis for events other than type II-P.

2.2. The prediction of CITE agrees with observations

A primary prediction of CITE is that E_{kin} increases with the mass of the progenitor (Kushnir 2015). This is more apparent by considering the binding energy of the shells to be ejected, E_{bin} (corrected for thermal energy), which is more negative for more massive progenitors. We can write quite generally that E_{kin} is given by

$$E_{\text{kin}} \approx E_{\text{dep}} + E_{\text{bin}}, \quad (1)$$

where E_{dep} is the energy deposited in the ejecta. For CITE, the deposited energy is thermonuclear, $E_{\text{dep}} \sim M_{\text{shell}} \times \text{MeV}/m_p$, where M_{shell} is the mass of shell of the thermonuclear fuel (the explosive shell). The relevant binding energy in this case is the one exterior to the base of the explosive shell, $E_{\text{bin}} \sim -GM_{\text{base}}M_{\text{shell}}/r_{\text{base}}$, where M_{base} and r_{base} are the enclosed mass and the radius at the base of the explosive shell, respectively. E_{dep} and $|E_{\text{bin}}|$ are comparable, since $\text{few} \times GM_{\text{base}}/r_{\text{base}} \approx \text{MeV}/m_p$ (Kushnir & Katz 2014). Therefore, E_{kin} can never exceeds significantly $|E_{\text{bin}}|$, and in the absence of a tuning between E_{dep} and E_{bin} , E_{kin} cannot be much smaller than $|E_{\text{bin}}|$. Therefore, $E_{\text{kin}} \sim |E_{\text{bin}}|$ for CITE. This order of magnitude estimate is validated in panel (b) of Figure 1, which shows the results of the CITE simulations that exploded successfully from Kushnir (2015). The conclusion is that the prediction of CITE agrees with the observation that more massive progenitors lead to stronger explosions.

2.3. The prediction of the neutrino mechanism possibly contradicts observations

For the neutrino mechanism, E_{dep} is the energy deposited by neutrinos. Since from basic considerations the iron core is

similar over a wide range of progenitor masses (the iron core is approximately a Chandrasekhar-mass white dwarf), E_{dep} is roughly constant over a wide progenitor mass range. However, the relevant binding energy in this case, the one exterior to the iron core, changes significantly between different progenitor masses. Therefore, as long as $E_{\text{dep}} \gg |E_{\text{bin}}|$, Equation (1) predicts that $E_{\text{kin}} \approx E_{\text{dep}} \approx \text{constant}$. At some progenitor mass E_{dep} is comparable to $|E_{\text{bin}}|$, such that for higher progenitor masses the explosion fails, since the deposited energy by neutrinos is smaller than the (absolute) binding energy. This behavior should be general for the neutrino mechanism, and probably does not depend on the specific scenario in which the star explodes. In fact, this behavior should hold for every scenario in which the deposited energy is dominated by the stellar core and is not sensitive to the binding energy of the shells to be ejected. So we expect E_{kin} to be constant up to some value of $|E_{\text{bin}}|$ (threshold progenitor mass) and then to rapidly fall to zero (failed explosions).

The results of Ugliano et al. (2012) for the neutrino mechanism are shown in Panel (c) of Figure 1. I use the values of E_{bin} , as reported by Ugliano et al. (2012), which are defined exterior to the iron core (at a mass coordinate of $\approx 1.5 M_{\odot}$), and are approximately the binding energies of the shells that are to be ejected. At low progenitor masses (low $|E_{\text{bin}}|$) the value of E_{kin} is indeed constant. However, instead of a sharp drop for E_{kin} at some value of $|E_{\text{bin}}|$, there is a complicated behavior near $|E_{\text{bin}}| \approx 10^{51}$ erg, which received much attention recently (O’Connor & Ott 2011; Ugliano et al. 2012; Pejcha & Thompson 2015; Ertl et al. 2015). The range of binding energies over which this complicated behavior is obtained is only a factor of ≈ 2 and is of no importance for the current discussion. Another complication in the behavior for the neutrino mechanism is the predicted weak explosions ($\approx 10^{50}$ erg) for the lowest mass progenitors (electron-capture supernova (ECSN); Nomoto 1984, 1987; Kitaura et al. 2006; Janka et al. 2008; Wanajo et al. 2011). However, the combination of two different mechanisms (iron core-collapse at high progenitor masses and electron-capture at low progenitor masses) is not supported by the uniformity of the observed correlations for the entire progenitor mass range (see the discussion at the end of Section 3.2). In summary, the prediction of the neutrino mechanism is a roughly constant E_{kin} for a wide range of progenitor masses and a sharp drop (maybe with a complicated behavior over a small range of progenitor masses) at some progenitor mass. This is in a possible contradiction with the observation that more massive progenitors lead to stronger explosions. It is yet to be seen whether accurate three-dimensional simulations of the neutrino mechanism, with all relevant physical process taken into account, would reproduce this observation.

3. EJECTED ^{56}Ni MASSES VERSUS THE KINETIC ENERGIES OF THE EJECTA

3.1. Observations

Estimates of E_{kin} and M_{Ni} for 70 observed supernovae within comoving radial distance of < 100 Mpc (to exclude rare events) are listed in Table 2 and are shown in Figure 3. This is the same compilation of Kushnir (2015) with a few more events. Note that the distribution of the sample in the $E_{\text{kin}}-M_{\text{Ni}}$ plane does not represent the relative rates of the events. A clear correlation over two orders of magnitude for both E_{kin} and M_{Ni} is apparent. Stronger explosions eject larger masses of ^{56}Ni . This correlation allowed the use of M_{Ni}

as an indicator for E_{kin} in Section 2. The estimates of E_{kin} from observations involve complicated light-curve modeling (which can include large systematic uncertainties). However, unlike the situation in Figure 2, in this case the sample is large and it spans more than two orders of magnitude in M_{Ni} and E_{kin} , such that the large systematic uncertainties are less important.

3.2. A common mechanism for all CCSNe

The correlation between E_{kin} and M_{Ni} holds for all types of CCSNe (types II and Ibc), and spans the entire observed ranges of E_{kin} ($\sim 10^{50} - 10^{52}$ erg) and M_{Ni} ($\sim 10^{-3} - 1 M_{\odot}$). This correlation suggests a common mechanism for all CCSNe, from the weakest observed explosions to the strongest ones. Such a common mechanism is predicted for CITE (Kushnir 2015), but seems unlikely for the neutrino mechanism, for two reasons. The first reason is that current simulations of the neutrino mechanism do not produce strong ($\sim 10^{52}$ erg) explosions (see the discussion in Janka 2012). The second reason is that weak ($\sim 10^{50}$ erg) explosions would require an extreme tuning for the neutrino mechanism. In the case that $|E_{\text{bin}}| \sim 10^{51}$ erg, the fraction of the gravitational energy ($\sim 10^{53}$ erg) released in neutrinos that is deposited should be $\sim 2\%$ for moderate ($\sim 10^{51}$ erg) explosions, and should be $\sim 1.1\%$ for weak explosions (a tuning of $\sim 10^{-3}$). In the case that $|E_{\text{bin}}| \sim 10^{50}$ erg, the fraction of the gravitational energy released in neutrinos that is deposited should be $\sim 0.2\%$ for weak explosions (again, a tuning of $\sim 10^{-3}$). The possibility that a different mechanism (ECSN) is operating for the lowest mass progenitors is not supported by the smooth observed correlations, which suggest a common mechanism for all CCSNe. This is demonstrated more robustly by the correlation between M_{Ni} and the V-band plateau luminosities, which suggests a common mechanism for weak and moderate events (Spiro et al. 2014, Figure 16 there).

3.3. The progenitors of type Ibc explosions are massive Wolf-Rayet (WR) stars – no deficit of high mass progenitors for CCSNe

The distribution of the different types of events in the $E_{\text{kin}}-M_{\text{Ni}}$ plane indicates that the sequence II-P, 87A like, IIb, Ibc is a sequence of E_{kin} and of M_{Ni} (this sequence is evident even when considering only M_{Ni} , which is more robustly observed).

E_{kin} and M_{Ni} for type Ibc explosions are larger by an order of a magnitude than E_{kin} and M_{Ni} for type II-P explosions, respectively. Let us consider the possibility that the progenitors of types Ibc and type II-P supernovae have a similar mass range, and that the different display of the supernova is solely because of the stripping of the hydrogen envelope for the type Ibc case. One expects that in this case E_{kin} and M_{Ni} would be similar for types II-P and Ibc, since these parameters are determined by the explosion mechanism, which takes place at the interior of the star, and is independent of the hydrogen envelope properties (and whether it exists or not). However, as pointed out above, E_{kin} and M_{Ni} for type Ibc explosions are larger by an order of a magnitude than the typical values for type II-P explosions. Therefore, the possibility that the progenitors of types Ibc and type II-P supernovae have a similar mass range is disfavored by observations.

One caveat is that ^{56}Ni -powered events like type Ibc are hard to find when M_{Ni} is small, while type II events that initially powered by shock cooling can be observed even if

they produce no ^{56}Ni at all. Therefore, the lack of type Ibc events with small values of M_{Ni} may be because of a selection bias. One possible way to check for such a bias is to calculate the (Pearson) partial correlation between $\log_{10}(E_{\text{kin}})$ and $\log_{10}(M_{\text{Ni}})$ given the distances to the events, which is $\rho \simeq 0.73$ with a p -value of $\simeq 1.4 \cdot 10^{-13}$, suggesting that such a bias is unlikely.

The second discussed possibility for the progenitors of type Ibc are Wolf-Rayet (WR) stars (see also the suggestion that the observed progenitor of the type Ib SN PTF13bvn is a WR star; Cao et al. 2013; Groh et al. 2013). Since these stars have more massive cores, CITE predicts that they lead to stronger explosions and larger amounts of ^{56}Ni are ejected. This continues the trend that was established in Section 2 for type II explosions, that more massive progenitors yield stronger explosions. One argument given by Bersten et al. (2014) and by Smartt (2015) against WR stars being the progenitors of type Ibc is the low estimated mass of the ejecta (typically $1-4 M_{\odot}$) compared to the mass of WR stars (typically $8-20 M_{\odot}$). However, this is a problem only if one assumes that most of the mass of the progenitor is ejected, as predicted by the neutrino mechanism. For CITE, only the mass exterior to the base of the explosive shell is ejected, and in the case that there is no hydrogen envelope, this mass agrees with the estimated ejected mass from observations (Kushnir 2015). It is further predicted by CITE for WR progenitors that the interior mass to the base of the explosive shell collapses and forms a massive black hole. So, assuming CITE explosions, strong type Ibc explosions with low ejecta masses are consistent with massive WR progenitors. Progenitor studies that assume a similar mass range for the progenitors of types II-P and Ibc supernovae suggest a deficit of high mass progenitors ($\gtrsim 20 M_{\odot}$) for CCSNe (e.g., see Smartt 2009). However, If massive WR stars are the progenitors of type Ibc supernovae, there is no deficit of high mass progenitors for CCSNe (Smartt 2015).

In summary, the observational evidence suggests that the sequence II-P, 87A like, IIb, Ibc is a progenitor mass sequence, where more massive progenitors lead to stronger explosions.

I thank Subo Dong, Avishay Gal-Yam, Boaz Katz and Eran Ofek for useful discussions and for a thorough reading of the manuscript. D. K. gratefully acknowledges support from the Friends of the Institute for Advanced Study.

REFERENCES

Arcavi, I., Gal-Yam, A., Cenko, S. B., et al. 2012, ApJ, 756, L30

- Arnett, W. D., Bahcall, J. N., Kirshner, R. P., & Woosley, S. E. 1989, ARA&A, 27, 629
- Bersten, M. C., Benvenuto, O. G., Folatelli, G., et al. 2014, AJ, 148, 68
- Bethe, H. A. 1990, Reviews of Modern Physics, 62, 801
- Burbidge, E. M., Burbidge, G. R., Fowler, W. A., & Hoyle, F. 1957, Reviews of Modern Physics, 29, 547
- Cao, Y., Kasliwal, M. M., Arcavi, I., et al. 2013, ApJ, 775, L7
- Dall’Ora, M., Botticella, M. T., Pumo, M. L., et al. 2014, ApJ, 787, 139
- Ertl, T., Janka, H.-T., Woosley, S. E., Sukhbold, T., & Ugliano, M. 2015, arXiv:1503.07522
- Fowler, W. A., & Hoyle, F. 1964, ApJS, 9, 201
- Fraser, M., Ergon, M., Eldridge, J. J., et al. 2011, MNRAS, 417, 1417
- Groh, J. H., Georgy, C., & Ekström, S. 2013, A&A, 558, L1
- Hamuy, M., & Pinto, P. A. 2002, ApJ, 566, L63
- Hamuy, M. 2003, ApJ, 582, 905
- Hendry, M. A., Smartt, S. J., Maund, J. R., et al. 2005, MNRAS, 359, 906
- Hendry, M. A., Smartt, S. J., Crockett, R. M., et al. 2006, MNRAS, 369, 1303
- Hirata, K., Kajita, T., Koshiba, M., Nakahata, M., & Oyama, Y. 1987, Physical Review Letters, 58, 1490
- Hoyle, F., & Fowler, W. A. 1960, ApJ, 132, 565
- Huang, F., Wang, X., Zhang, J., et al. 2015, arXiv:1504.00446
- Insera, C., Turatto, M., Pastorello, A., et al. 2011, MNRAS, 417, 261
- Janka, H.-T., Müller, B., Kitaura, F. S., & Buras, R. 2008, A&A, 485, 199
- Janka, H.-T. 2012, Annual Review of Nuclear and Particle Science, 62, 407
- Jerkstrand, A., Smartt, S. J., Sollerman, J., et al. 2015, MNRAS, 448, 2482
- Kitaura, F. S., Janka, H.-T., & Hillebrandt, W. 2006, A&A, 450, 345
- Kushnir, D., & Katz, B. 2014, arXiv:1412.1096
- Kushnir, D. 2015, arXiv:1502.03111
- Leonard, D. C. 2011, Ap&SS, 336, 117
- Lyman, J., Bersier, D., James, P., et al. 2014, arXiv:1406.3667
- Maund, J. R., Smartt, S. J., Kudritzki, R. P., Podsiadlowski, P., & Gilmore, G. F. 2004, Nature, 427, 129
- Morales-Garoffolo, A., Elias-Rosa, N., Benetti, S., et al. 2014, MNRAS, 445, 1647
- Nomoto, K. 1984, ApJ, 277, 791
- Nomoto, K. 1987, ApJ, 322, 206
- Nugent, P., Sullivan, M., Ellis, R., et al. 2006, ApJ, 645, 841
- O’Connor, E., & Ott, C. D. 2011, ApJ, 730, 70
- Pastorello, A., Baron, E., Branch, D., et al. 2005, MNRAS, 360, 950
- Pastorello, A., Pumo, M. L., Navasardyan, H., et al. 2012, A&A, 537, AA141
- Pejcha, O., & Thompson, T. A. 2015, ApJ, 801, 90
- Poznanski, D., Butler, N., Filippenko, A. V., et al. 2009, ApJ, 694, 1067
- Poznanski, D. 2013, MNRAS, 436, 3224
- Smartt, S. J. 2009, ARA&A, 47, 63
- Smartt, S. J., Eldridge, J. J., Crockett, R. M., & Maund, J. R. 2009, MNRAS, 395, 1409
- Smartt, S. J. 2015, PASA, 32, e016
- Spiro, S., Pastorello, A., Pumo, M. L., et al. 2014, MNRAS, 439, 2873
- Taddia, F., Stritzinger, M. D., Sollerman, J., et al. 2012, A&A, 537, AA140
- Takáts, K., Pignata, G., Pumo, M. L., et al. 2015, MNRAS, 450, 3137
- Tomasella, L., Cappellaro, E., Fraser, M., et al. 2013, MNRAS, 434, 1636
- Ugliano, M., Janka, H.-T., Marek, A., & Arcones, A. 2012, ApJ, 757, 69
- Utrobin, V. P., & Chugai, N. N. 2014, arXiv:1411.6480
- van Dyk, S. D. 1992, AJ, 103, 1788
- Wanajo, S., Janka, H.-T., Müller, B. 2011, ApJ, 726, L15

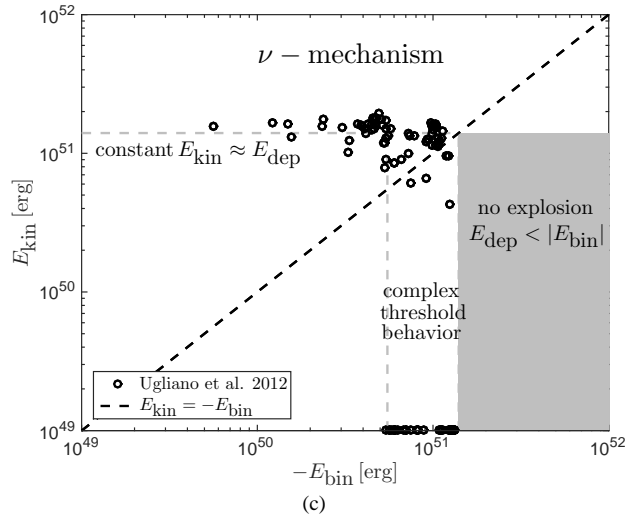
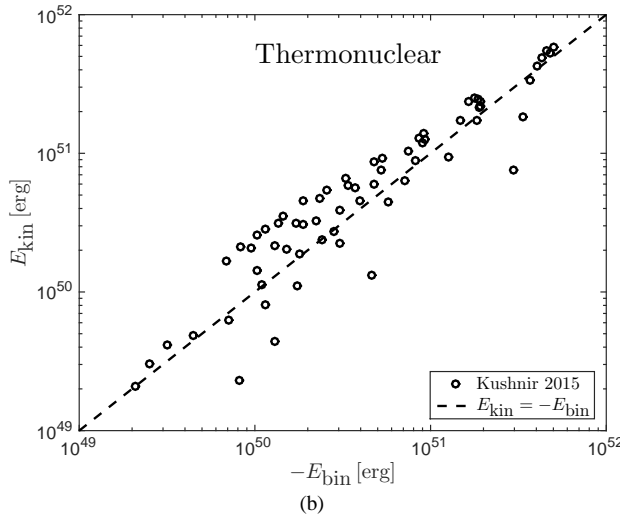
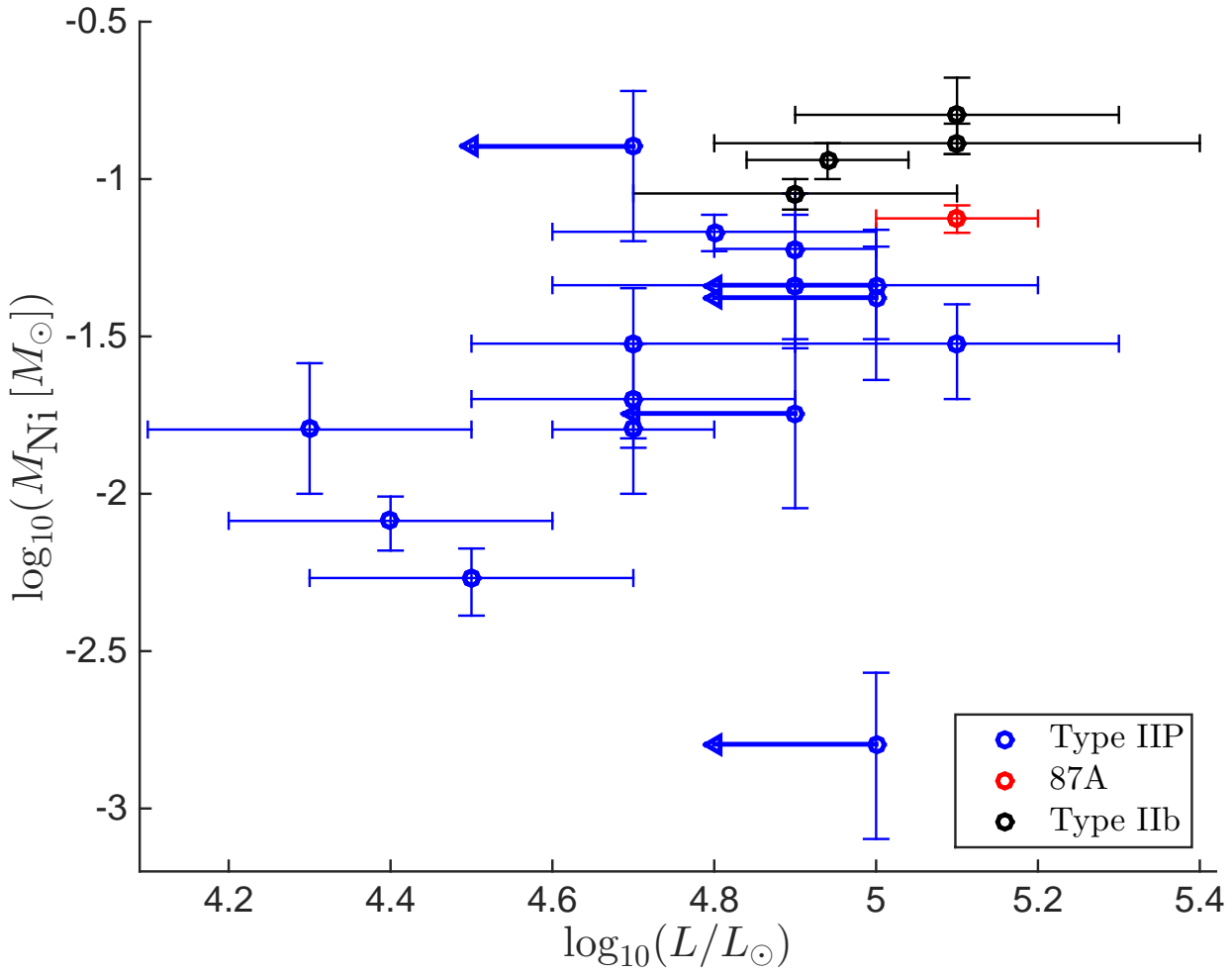


Figure 1. Panel (a): The observed correlation between M_{Ni} and the luminosities of the progenitors for type II supernovae, which was first reported by Fraser et al. (2011), is reproduced here with updated data. The sample includes all supernovae from Smartt (2015), for which an estimate of M_{Ni} is available in the literature, supplemented with SN 1987A and SN 1993J (see Table 1). In the cases that M_{Ni} lacks an error estimate, an error of 50% was assumed (10% for SN 1987A). More luminous progenitors eject larger masses of ^{56}Ni . Since more luminous progenitors are more massive (with more negative binding energy, E_{bin}) and since larger values of M_{Ni} imply larger E_{kin} (see Section 3 and Figure 3), the correlation implies that more massive progenitors lead to stronger explosions. The range of M_{Ni} roughly corresponds to $E_{\text{kin}} \sim \text{few} \times 10^{50} - \text{few} \times 10^{51}$ erg. Panel (b): The kinetic energy of the ejecta as function of E_{bin} at the base of the explosive shell for the CITE simulations that exploded successfully from Kushnir (2015). Panel (c): The kinetic energy of the ejecta as function of E_{bin} exterior to the iron core for the neutrino mechanism simulations of Ugliano et al. (2012). The points at 10^{49} erg represent failed explosions.

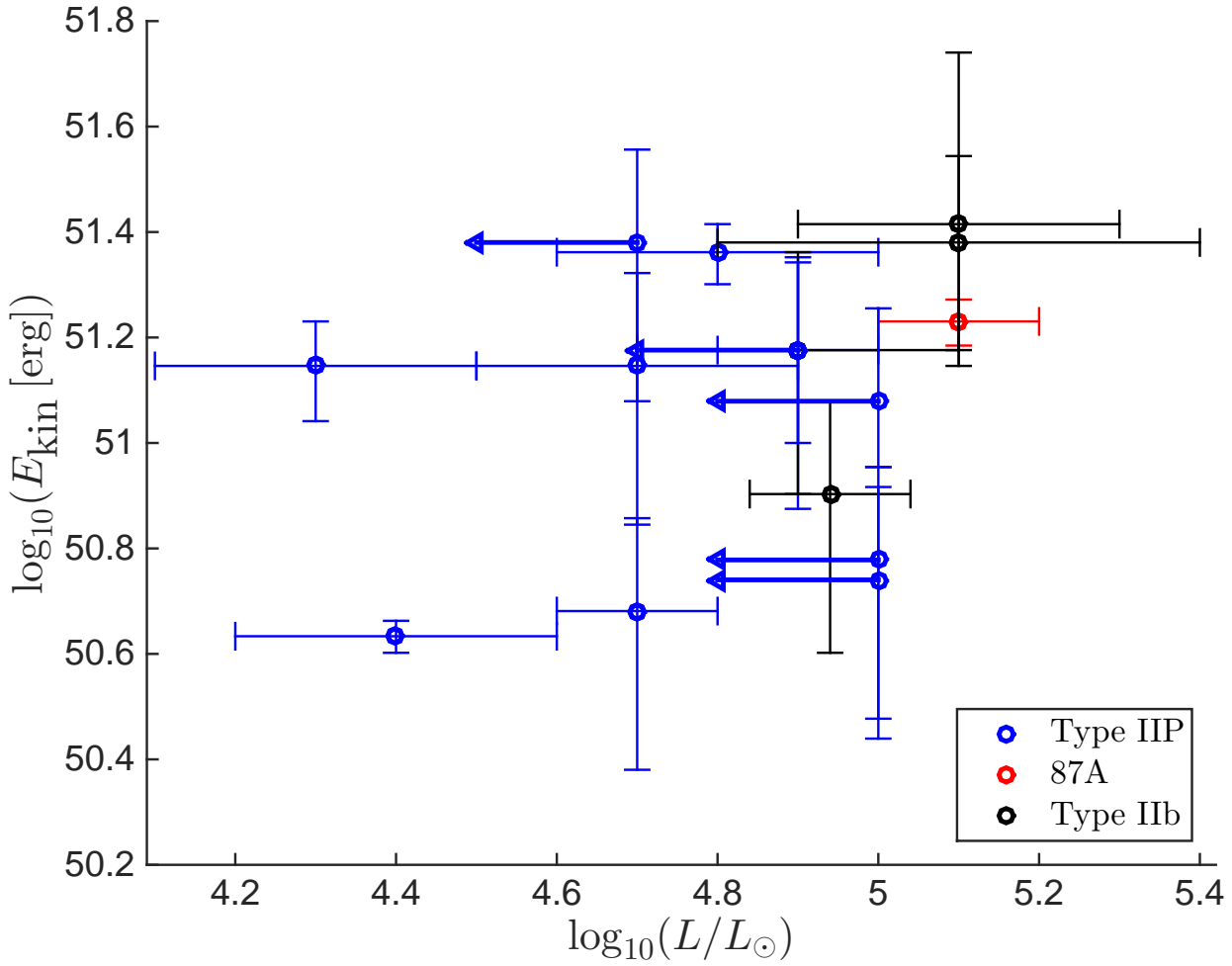


Figure 2. The observed correlation between the estimated E_{kin} and the luminosities of the progenitors. The sample includes all supernovae from Smartt (2015), for which an estimate of E_{kin} is available in the literature, supplemented with SN 1987A and SN 1993J (see Table 1). In the cases that E_{kin} lacks an error estimate, an error of 50% was assumed (10% for SN 1987A). The estimates of E_{kin} from observations involve complicated light-curve modeling (which can include large systematic uncertainties). This is probably the reason for the weak observed correlation that is obtained when using E_{kin} compared to the strong observed correlation that is obtained when using M_{Ni} (panel (a) of Figure 1), which is model-free and can be directly derived from observations.

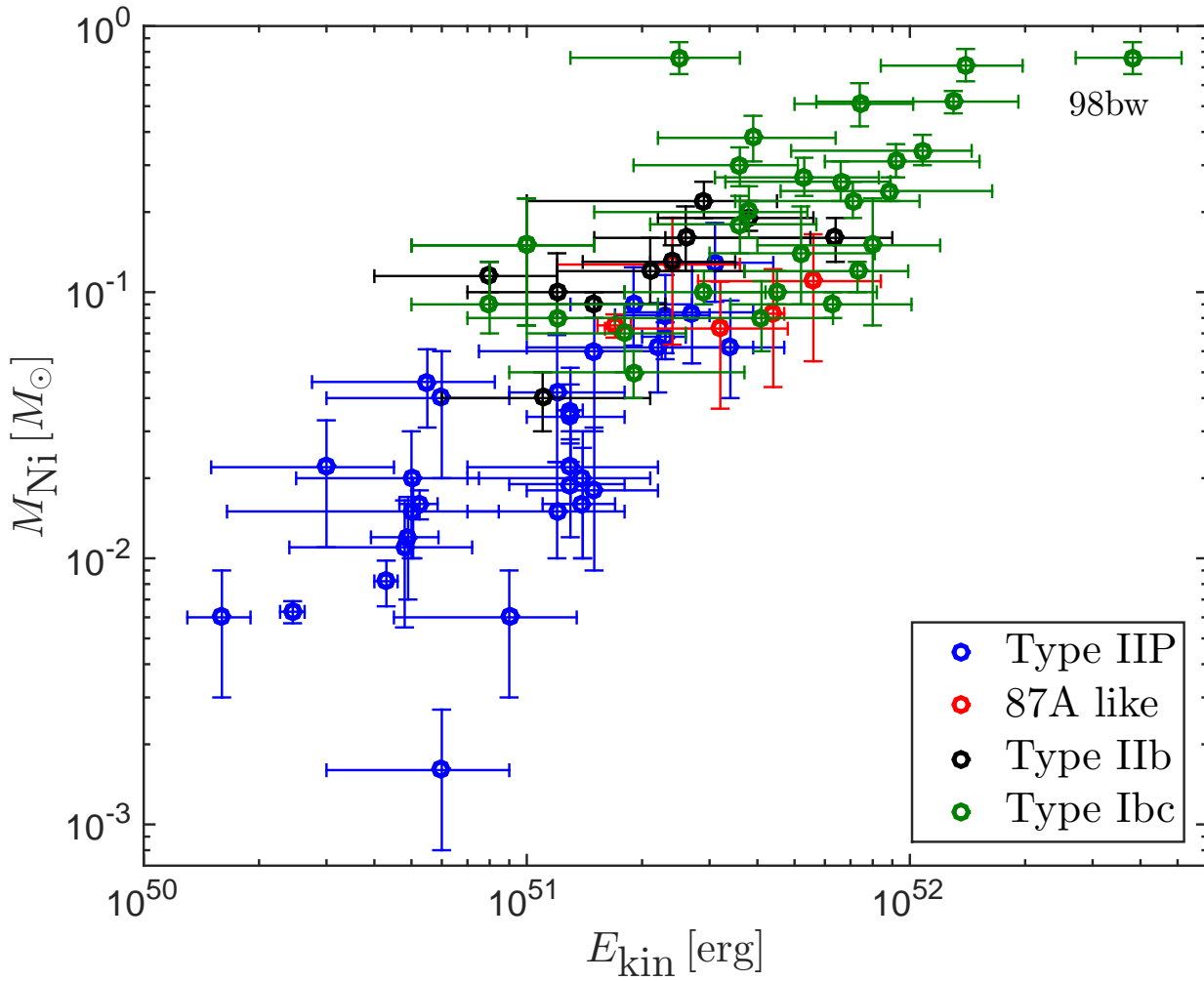


Figure 3. Estimates of E_{kin} and M_{Ni} from the literature for 70 observed supernovae (see Table 2). This is the same compilation of Kushnir (2015) with a few more events. In the case that E_{kin} or M_{Ni} lack an error estimate, an error of 50% was assumed (10% for SN 1987A). The estimates of E_{kin} from observations involve complicated light-curve modeling (which can include large systematic uncertainties). However, unlike the situation in Figure 2, in this case the sample is large and it spans more than two orders of magnitude in M_{Ni} and E_{kin} , such that the large systematic uncertainties are less important.

Table 1

The progenitors from the sample of Smartt (2015), for which estimates of M_{Ni} are available in the literature, supplemented with SN 1987A and SN 1993J.

Name	$\log_{10}(L/L_{\odot})$	$E_{\text{kin}} [10^{51} \text{ erg}]$	$^{56}\text{Ni mass } [M_{\odot}]$	Type
03gd	$4.3^{+0.2}_{-0.2}$	$1.4^{+0.3}_{-0.3}$	$0.016^{+0.01}_{-0.006}$	IIP
05cs	$4.4^{+0.2}_{-0.2}$	$0.43^{+0.03}_{-0.03}$	$0.0082^{+0.0016}_{-0.0016}$	IIP
09md	$4.5^{+0.2}_{-0.2}$	–	$0.0054^{+0.0013}_{-0.0013}$	IIP
06my	$4.7^{+0.2}_{-0.2}$	–	$0.03^{+0.015}_{-0.015}$	IIP
12A	$4.7^{+0.1}_{-0.1}$	0.48	$0.016^{+0.002}_{-0.002}$	IIP
13ej	$4.7^{+0.2}_{-0.2}$	$1.4^{+0.7}_{-0.7}$	$0.02^{+0.01}_{-0.01}$	IIP
04et	$4.8^{+0.2}_{-0.2}$	$2.3^{+0.3}_{-0.3}$	$0.068^{+0.009}_{-0.009}$	IIP
04A	$4.9^{+0.3}_{-0.3}$	–	$0.046^{+0.031}_{-0.017}$	IIP
12aw	$4.9^{+0.1}_{-0.1}$	1.5	0.06	IIP
12ec	$5.1^{+0.2}_{-0.2}$	–	$0.03^{+0.01}_{-0.01}$	IIP
06ov	< 4.7	2.4	0.127	IIP
99gi	< 4.9	$1.5^{+0.7}_{-0.5}$	$0.018^{+0.013}_{-0.009}$	IIP
99br	< 5	0.6	$0.0016^{+0.0011}_{-0.0008}$	IIP
99em	< 5	$1.2^{+0.6}_{-0.3}$	$0.042^{+0.027}_{-0.019}$	IIP
09ib	< 5	0.55	$0.046^{+0.015}_{-0.015}$	IIP
08ax	$5.1^{+0.2}_{-0.2}$	$2.6^{+2.9}_{-1.1}$	$0.16^{+0.05}_{-0.04}$	IIb
11dh	$4.9^{+0.2}_{-0.2}$	$1.5^{+0.8}_{-0.7}$	$0.09^{+0.01}_{-0.01}$	IIb
13df	$4.94^{+0.1}_{-0.1}$	$0.8^{+0.4}_{-0.4}$	$0.115^{+0.015}_{-0.015}$	IIb
87A	$5.1^{+0.1}_{-0.1}$	1.7	0.075	87A
93J	$5.1^{+0.3}_{-0.3}$	$2.4^{+1.1}_{-1}$	$0.13^{+0.02}_{-0.01}$	IIb

Note. — The luminosities of the progenitors are from Smartt (2015), except SN 1987A (Smartt et al. 2009) and SN 1993J (Maund et al. 2004). The estimates of E_{kin} and of M_{Ni} are from Table 2, except SN 2009md (Fraser et al. 2011), SN 2006my (Smartt et al. 2009), SN 2004A (Hendry et al. 2006) and SN 2012ec (Jerkstrand et al. 2015).

Table 2
A compilation from the literature of estimated E_{kin} and M_{Ni} from the light-curves.

Name	Kinetic energy [10^{51} erg]	^{56}Ni mass [M_{\odot}]	Type	Reference	Name	Kinetic energy [10^{51} erg]	^{56}Ni mass [M_{\odot}]	Type	Reference
69L	$2.3^{+0.7}_{-0.6}$	$0.082^{+0.034}_{-0.026}$	IIP	3	73R	$2.7^{+1.2}_{-0.9}$	$0.084^{+0.044}_{-0.03}$	IIP	3
83I	1	0.15	Ibc	3	83N	1	0.15	Ibc	3
84L	1	0.15	Ibc	3	86L	$1.3^{+0.5}_{-0.3}$	$0.034^{+0.018}_{-0.011}$	IIP	3
87A	1.7	0.075	87A	3	88A	$2.2^{+1.7}_{-1.2}$	$0.062^{+0.029}_{-0.02}$	IIP	3
89L	$1.2^{+0.6}_{-0.5}$	$0.015^{+0.008}_{-0.005}$	IIP	3	90E	$3.4^{+1.3}_{-1}$	$0.062^{+0.031}_{-0.022}$	IIP	3
91G	$1.3^{+0.9}_{-0.6}$	$0.022^{+0.008}_{-0.006}$	IIP	3	92H	$3.1^{+1.3}_{-1}$	$0.129^{+0.053}_{-0.037}$	IIP	3
92ba	$1.3^{+0.5}_{-0.4}$	$0.019^{+0.009}_{-0.007}$	IIP	3	93J	$2.4^{+1.1}_{-1}$	$0.13^{+0.02}_{-0.01}$	Ib	11
94I	$1.2^{+0.6}_{-0.5}$	$0.08^{+0.01}_{-0.01}$	Ibc	11	96cb	$2.1^{+1.6}_{-0.9}$	$0.12^{+0.04}_{-0.03}$	Ib	11
97D	0.9	0.006	IIP	3	97ef	8	0.15	Ibc	3
98A	5.6	0.11	87A	7	98bw	$38.2^{+13}_{-11.1}$	$0.76^{+0.11}_{-0.1}$	Ibc	11
99br	0.6	$0.0016^{+0.0011}_{-0.0008}$	IIP	3	99cr	$1.9^{+0.8}_{-0.6}$	$0.09^{+0.034}_{-0.027}$	IIP	3
99dn	$7.3^{+2.6}_{-3.6}$	0.12	Ibc	11	99em	$1.3^{+0.1}_{-0.1}$	$0.036^{+0.009}_{-0.009}$	IIP	1
99em	$1.2^{+0.6}_{-0.3}$	$0.042^{+0.027}_{-0.019}$	IIP	3	99ex	$3.6^{+2.1}_{-1.5}$	$0.18^{+0.05}_{-0.04}$	Ibc	11
99gi	$1.5^{+0.7}_{-0.5}$	$0.018^{+0.013}_{-0.009}$	IIP	3	00cb	$4.4^{+0.3}_{-0.3}$	$0.083^{+0.039}_{-0.039}$	87A	1
02ap	$6.3^{+3.8}_{-2.9}$	$0.09^{+0.01}_{-0.01}$	Ibc	11	03Z	$0.245^{+0.018}_{-0.018}$	$0.0063^{+0.0006}_{-0.0006}$	IIP	4
03bg	$3.8^{+1.8}_{-1.6}$	$0.19^{+0.03}_{-0.02}$	Ib	11	03gd	$1.4^{+0.3}_{-0.3}$	$0.016^{+0.01}_{-0.006}$	IIP	5
03jd	$7.4^{+2.8}_{-2.4}$	$0.51^{+0.1}_{-0.09}$	Ibc	11	04aw	$6.6^{+2.3}_{-3.3}$	$0.26^{+0.05}_{-0.04}$	Ibc	11
04dk	$5.3^{+3}_{-2.2}$	$0.27^{+0.05}_{-0.04}$	Ibc	11	04dn	$7.1^{+3.5}_{-3.6}$	$0.22^{+0.04}_{-0.03}$	Ibc	11
04et	$2.3^{+0.3}_{-0.3}$	$0.068^{+0.009}_{-0.009}$	IIP	1	04fe	$3.6^{+1.5}_{-1.7}$	$0.3^{+0.05}_{-0.05}$	Ibc	11
04ff	$2.9^{+1.6}_{-1.9}$	$0.22^{+0.04}_{-0.03}$	Ib	11	04gq	$5.2^{+2.9}_{-2.2}$	$0.14^{+0.07}_{-0.05}$	Ibc	11
05az	$3.9^{+2.5}_{-1.7}$	$0.38^{+0.08}_{-0.07}$	Ibc	11	05bf	$0.8^{+1.4}_{-0.3}$	$0.09^{+0.04}_{-0.02}$	Ibc	11
05cs	$0.43^{+0.03}_{-0.03}$	$0.0082^{+0.0016}_{-0.0016}$	IIP	1	05cs	$0.16^{+0.03}_{-0.03}$	$0.006^{+0.003}_{-0.003}$	IIP	2
05hg	$2.5^{+1.1}_{-1.2}$	$0.76^{+0.11}_{-0.1}$	Ibc	11	06T	$1.2^{+0.6}_{-0.5}$	$0.1^{+0.04}_{-0.02}$	Ib	11
06au	3.2	0.073	87A	8	06el	$6.4^{+2.6}_{-4.1}$	$0.16^{+0.03}_{-0.03}$	Ib	11
06ep	$4.1^{+2.2}_{-2.4}$	$0.08^{+0.03}_{-0.02}$	Ibc	11	06ov	2.4	0.127	87A	8
07C	$3.8^{+1.6}_{-2.3}$	$0.2^{+0.05}_{-0.04}$	Ibc	11	07Y	$1.9^{+1.8}_{-1}$	$0.05^{+0.01}_{-0.01}$	Ibc	11
07gr	$2.9^{+1.3}_{-1.1}$	$0.1^{+0.02}_{-0.01}$	Ibc	11	07od	0.5	0.02	IIP	6
07ru	$13^{+6.2}_{-7.3}$	$0.52^{+0.05}_{-0.05}$	Ibc	11	07uy	$10.8^{+3.7}_{-5.9}$	$0.34^{+0.05}_{-0.04}$	Ibc	11
08D	$4.5^{+3.7}_{-1.7}$	$0.1^{+0.02}_{-0.01}$	Ibc	11	08ax	$2.6^{+2.9}_{-1.1}$	$0.16^{+0.05}_{-0.04}$	Ib	11
08in	$0.505^{+0.34}_{-0.34}$	$0.015^{+0.005}_{-0.005}$	IIP	1	08in	$0.49^{+0.098}_{-0.098}$	$0.012^{+0.005}_{-0.005}$	IIP	2
09E	0.6	0.04	IIP	7	09bb	$9.2^{+6}_{-3.2}$	$0.31^{+0.05}_{-0.04}$	Ibc	11
09bw	0.3	0.022	IIP	10	09ib	0.55	$0.046^{+0.015}_{-0.015}$	IIP	12
09jf	$8.9^{+7.5}_{-4.3}$	$0.24^{+0.03}_{-0.02}$	Ibc	11	11bm	$14^{+5.7}_{-5.6}$	$0.71^{+0.11}_{-0.09}$	Ibc	11
11dh	$1.5^{+0.8}_{-0.7}$	$0.09^{+0.01}_{-0.01}$	Ib	11	11hs	$1.1^{+1}_{-0.5}$	$0.04^{+0.01}_{-0.01}$	Ib	11
12A	0.48	0.011	IIP	9	12A	$0.525^{+0.06}_{-0.06}$	$0.016^{+0.002}_{-0.002}$	IIP	1
12aw	1.5	0.06	IIP	10	13df	$0.8^{+0.4}_{-0.4}$	$0.115^{+0.015}_{-0.015}$	Ib	13
13ej	$1.4^{+0.7}_{-0.7}$	$0.02^{+0.01}_{-0.01}$	IIP	14	iPTF13bvn	$1.8^{+0.8}_{-0.8}$	$0.07^{+0.02}_{-0.02}$	Ibc	11

Note. — REFERENCES.—(1) Utrobin & Chugai (2014);(2) Spiro et al. (2014);(3) Hamuy (2003);(4) Hendry et al. (2005);(5) Inserra et al. (2011);(6) Pastorello et al. (2012);(7) Pastorello et al. (2005);(8) Taddia et al. (2012);(9) Tomasella et al. (2013);(10) Dall’Ora et al. (2014);(11) Lyman et al. (2014); (12) Takáts et al. (2015); (13) Morales-Garoffolo et al. (2014); (14) Huang et al. (2015)